Nuclear Engineering and Technology 55 (2023) 3030–3038

Contents lists available at ScienceDirect

Nuclear Engineering and Technology

journal homepage: www.elsevier.com/locate/net

Original Article

ACA: Automatic search strategy for radioactive source

Jianwen Huo [a], Xulin Hu [a, *], Junling Wang [b], Li Hu [a]

[a] School of Information Engineering, Southwest University of Science and Technology, Mianyang, 621010, China
[b] School of National Defense Science, Southwest University of Science and Technology, Mianyang, 621010, China

ARTICLE INFO

Article history:
Received 26 November 2022
Received in revised form
1 April 2023
Accepted 14 May 2023
Available online 20 June 2023

Keywords:
Radioactive source search
Source location estimation
Path planning
Occupancy grid map
Monte Carlo

ABSTRACT

Nowadays, mobile robots have been used to search for uncontrolled radioactive source in indoor environments to avoid radiation exposure for technicians. However, in the indoor environments, especially in the presence of obstacles, how to make the robots with limited sensing capabilities automatically search for the radioactive source remains a major challenge. Also, the source search efficiency of robots needs to be further improved to meet practical scenarios such as limited exploration time. This paper proposes an automatic source search strategy, abbreviated as ACA: the location of source is estimated by a convolutional neural network (CNN), and the path is planned by the A-star algorithm. First, the search area is represented as an occupancy grid map. Then, the radiation dose distribution of the radioactive source in the occupancy grid map is obtained by Monte Carlo (MC) method simulation, and multiple sets of radiation data are collected through the eight neighborhood self-avoiding random walk (ENSAW) algorithm as the radiation data set. Further, the radiation data set is fed into the designed CNN architecture to train the network model in advance. When the searcher enters the search area where the radioactive source exists, the location of source is estimated by the network model and the search path is planned by the A-star algorithm, and this process is iterated continuously until the searcher reaches the location of radioactive source. The experimental results show that the average number of radiometric measurements and the average number of moving steps of the ACA algorithm are only 2.1% and 33.2% of those of the gradient search (GS) algorithm in the indoor environment without obstacles. In the indoor environment shielded by concrete walls, the GS algorithm fails to search for the source, while the ACA algorithm successfully searches for the source with fewer moving steps and sparse radiometric data.

1. Introduction

With the popularization and application of nuclear power plants and irradiation industries worldwide, as well as the extensive development of nuclear facilities decommissioning and nuclear waste disposal, the risk of loss of radioactive source is gradually increasing. In the event of loss of radioactive source, it is necessary to search for radioactive source as soon as possible to avoid social panic and casualties [1]. Early source localization methods mainly relied on deploying a large number of sensor nodes in a radiation environment to build a sensor network. Then, based on a large amount of observation data obtained by the sensor nodes, the location of radioactive source is estimated by using the geometric method [2,3] and the least square method [4,5]. For example, Rao et al. used three nuclear radiation detectors to build a fixed sensor network, and then estimated the location of low-level point radioactive source in an open area by geometric method [3]. Howse et al. deployed four nuclear radiation detectors in the room to form a sensor network, and then used the least square method to estimate the location of mobile radioactive source in real time [4]. The maximum likelihood estimation method [6–8] has also been used to estimate the number of sources and the source term parameters by discrete radiation data from multiple detectors. In practical applications, the number of radiation measurements usually needs to be as few as possible due to the limited detection time. With advances in robotics, mobile robots carrying detectors have gradually been used to search for unknown radioactive sources due to their low risk, high search efficiency and source localization accuracy.

Bayesian estimation methods [9–12] are commonly applied to estimate source parameters. According to Bayesian theory, the posterior probability distribution of the source parameter vector which can be approximated by the Markov chain Monte Carlo (MCMC) [9], particle filter [10,11] and importance sampling [12]

* Corresponding author.
E-mail address: xulinhu_zhang@163.com (X. Hu).

https://doi.org/10.1016/j.net.2023.05.017

methods is constructed from the radiation data obtained by the detectors. By solving the posterior probability distribution, the source parameters of radioactive source can be obtained. Huo J et al. designed an automatic robot search algorithm by using the partially observable Markov decision process (POMDP), and studied the improved MCMC method based on the Bayesian framework to realize the parameter estimation of radioactive source [9]. Liu et al. [10]studied an unscented particle filtering algorithm based on divide-and-conquer sampling to improve the search accuracy of radioactive source. Gao et al. [11] proposed the peak suppressed particle filter method which can handle multi-modal estimation problems in a mixed radiation field with sparse measurement data. Interpolation algorithms have also been applied to localize unknown radioactive sources by reconstructing 2D or 3D radiation dose rate fields. West A et al. [13] studied the reconstruction of 2D radiation distribution map of single radioactive source by Gaussian process regression method. They estimated the source parameters by using a mobile robot equipped with a compact $CeBr_3$ scintillator detector and a laser range sensor. Xie X et al. [14] designed a net function interpolation method, which can reconstruct the 3D radiation dose rate field based on sparse measurement data in a three-dimensional space with concrete walls and locate unknown radioactive sources. In addition, gamma cameras have also been studied for source parameter estimation by recording the number and direction of incident photons [15,16]. In Ref. [15], Tomita H et al. developed a path planning system based on 4 π gamma imaging to predict the next measurement position of mobile robot, and estimated the source parameters through the random forest algorithm.

With the development of artificial intelligence, machine learning methods such as supervised learning and reinforcement learning have been gradually applied to the research of source search [17–20]. Liu Z et al. [17] proposed to use convolutional neural network to plan the next measurement position of the detector, and combine the double Q-learning algorithm to complete the radiation source search task. Fathi A et al. [18] designed a network architecture similar to "Lenet-5″, which can quickly locate the lost gamma source by collecting sparse energy deposition data. Zhao Y et al. [19] used deep reinforcement learning (DRL) techniques to extract the feature of belief state, and introduced the deep Q-network (DQN) algorithm in the source search process to make optimal decisions. Proctor P et al. [20] presented a novel neural network architecture based on the advantage actor critic (A2C) framework to search for radiation sources in the non-convex environment. In addition, it is a good idea to represent the search area with an occupancy grid map, which is helpful for mobile robot to avoid obstacles and plan walking paths during the search process [13,21,22]. For example, Ji Y et al. [22] introduced an occupancy grid map to study the path planning of four-neighbor search A-star algorithm when searching for odor source. It is worth noting that the Monte Carlo (MC) method is also widely used in numerical simulations to simulate the physical process of particle transport in matter. A large number of simulation programs based on the MC method such as Geant4, MCNP and FLUKA have also been developed and gradually improved [23–25].

Due to limited exploration time, the searcher searching for radioactive sources in indoor environments often has to make effective motion decisions at current state with limited sensing capabilities and instantly available information [22]. However, existing source search methods have certain limitations and face several new challenges under such conditions. On the one hand, the searcher has to estimate the source location accurately as early as possible, and make appropriate global path planning at the current position to improve the efficiency of source search. The searcher can only obtain sparse radiation data within a limited exploration time, which requires a suitable source parameter estimation method to estimate the location or orientation of the source. On the other hand, in indoor environments, there may be obstacles in the area around unknown radioactive source, which may provide confusing information to the searcher and cause the source search to fail.

To address these challenges, this paper proposes an efficient **A**utomatic source search strategy (i.e. ACA algorithm) based on **C**onvolution neural network and **A**-star, which is suitable for both indoor environments without and with obstacles. The main contributions of this paper are as follows:

(1) This paper introduces an occupancy grid map to represent the search area. On this basis, the eight-neighbor search A-star algorithm is used to plan the global path of the current state to make the effective movement decisions and avoid obstacles in the indoor environment.
(2) CNN is employed as the source parameter estimation model which can estimate the direction and location of the source with sparse radiation data in indoor environments without and with obstacles. We take estimated source location as the searching target, which provides the searcher with a globally optimal solution for the current state.
(3) This paper proposes an automatic source search algorithm through an iterative search process: source location estimation, path planning. Verification experiments show that the proposed algorithm is superior to the GS algorithm in terms of the number of moving steps, the number of radiation measurements and the search success rate.

This paper is organized as follows: Section 2 introduces the radioactive source search task, search environment grid division, source parameter estimation model based on CNN, and path planning based on A-star algorithm. Section 3 carries out the simulation experiments of radioactive source search in indoor environments without and with obstacles, and analyzes the performance of the ACA algorithm. Section 4 concludes the paper and discusses possible future steps.

2. Problem formulation

2.1. Source search task description

Consider an indoor scene with an area of 10 m $\times$ 15 m. An isotropic γ radioactive source with an activity of 4 mCi and an energy of 2 MeV is lost in the indoor ground which is large enough relative to the radioactive source, and the distance between the detection plane of the searcher and the ground is h, as shown in plot (a) of Fig. 1. The ground is divided into 150 cells with 1 m $\times$ 1 m (the cell numbers are S1~S150 in sequence), and the radioactive source can be located in any of the 150 cells. Any location of the radioactive source within the cell is replaced by the central position of the cell. Subsequently, the search area is represented as an occupancy grid map with a resolution of 0.25 m (40 $\times$ 60 grids), and the center of grid represents the radiation measurement point, as shown in plot (b) of Fig. 1.

In order to obtain the radiation dose rate distribution of radioactive source in detection plane, the numerical simulation based on the MC method is carried out by Geant4 program. As shown in Fig. 2, the radiation dose rate distribution map of the radioactive

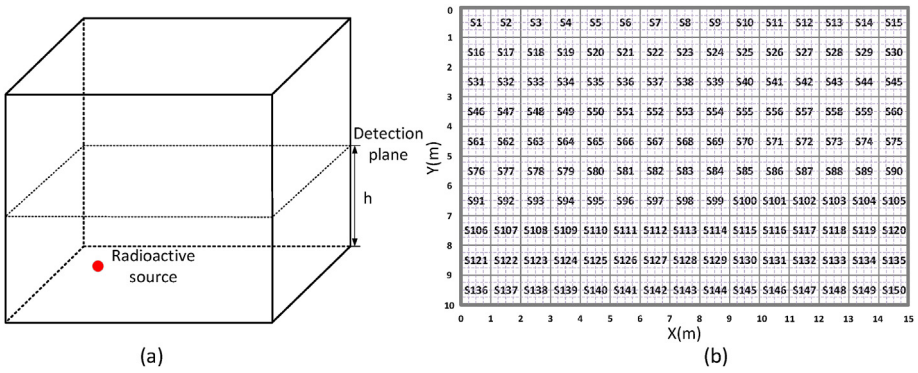

Fig. 1. (a) Description of radioactive source search problem. (b) The search area is represented by an occupancy grid map.

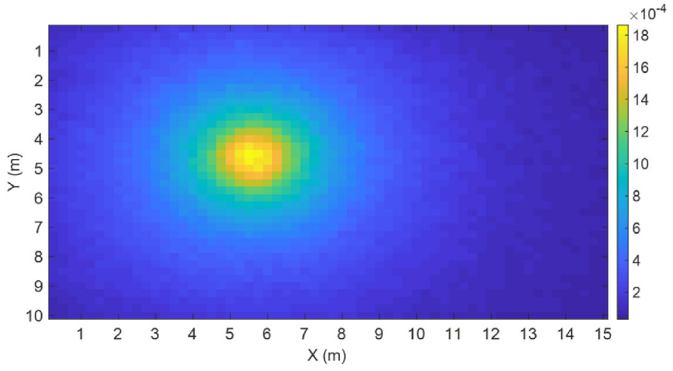

Fig. 2. Radiation dose rate distribution map of radioactive source (S66) at the height of 1 m above the ground (dose rate: μGy/s).

source (S66) at a height of $h = 1$ m above the ground is obtained by Geant4 approximation, and the calculation principle is as follows:

$$D = \frac{k \bullet dE}{\rho . dV} \tag{1}$$

where D is the air absorbed dose rate; E is the energy deposition of gamma rays in the air; V is the volume of air, ρ is the air density; k is the conversion factor for converting energy deposition into air absorbed dose rate. Similarly, the radiation dose rate distribution of radioactive source at different locations (S1~S150) at the height of $h = 1$ m above the ground can be approximated by the Geant4 program. In the source search task, the searcher has to find lost radioactive source with as few radiation detection times and moving steps as possible due to limited search time.

2.2. Radiation data acquisition

When the occupancy grid map is full of unoccupied grids, the searcher can move from the current state to any of the eight directions: up, down, left, right, southwest, northwest, northeast, and southeast. However, since there may be occupied grids in the occupancy grid map, the searcher only moves to the unoccupied grids and collects radiation data in the unoccupied grids. In order to obtain radiation dataset required by the source parameter estimation model, we use eight neighborhood self-avoiding random walk (ENSAW) algorithm to collect radiation data in the occupancy grid map. The ENSAW algorithm will randomly select an initial position in the occupied grid map at the beginning of collecting radiation data, and will not repeat the position it has already walked. In particular, it will bypass the occupied grid when walking (Fig. 3).

To reduce computational overhead of generating self-avoiding random walk paths, the method of weighted importance sampling is adopted [26]. Let $X_i = (x_i, y_i)$ represent the coordinate of step i of the n-step walk path ($1 \le i \le n, i \in Z$). Next, the probability mass function can be represented as

$$P(X_1, X_2, ..., X_n) = \frac{I((X_1, X_2, ..., X_n) \in E_n)}{Z_n} \tag{2}$$

where E_n is the set of n-step self-avoiding walk path; $I(\cdot)$ is the indicator function; Z_n is unknown. To select the next measurement point, a new probability mass function $Q(X_1, X_2, ..., X_n)$ is defined for weighted importance sampling. Suppose the number of unoccupied adjacent grids of X_{i-1} is d_{i-1} ($i \ge 2, i \in Z$). Since all information before the i-th step is known when predicting X_i, $Q(X_i | X_1, X_2, ..., X_{i-1})$ can be calculated by

$$Q(X_i | X_1, X_2, ..., X_{i-1}) = \begin{cases} 1/d_{i-1}, if X_i is unoccupied adjacent grid of X_{i-1} \\ 0, otherwise \end{cases} \tag{3}$$

Further, $X_1, X_2, ..., X_n$ will have a joint probability:

$$Q(X_1, X_2, ..., X_n) = \frac{I((X_1, X_2, ..., X_n) \in E_n)}{d_1 \cdots d_{n-1}} \tag{4}$$

Note that $(X_1, X_2, ..., X_n) \propto I((X_1, X_2, ..., X_n) \in E_n)$, the weight form can be represented as

$$W(X_1, X_2, ..., X_n) = I((X_1, X_2, ..., X_n) \in E_n) d_1 \cdots d_{n-1} \tag{5}$$

In this paper, radiation data is collected once every two steps in order to reduce the number of acquisition within the limited search time. For the radiation dose rate distribution maps corresponding to 150 different source locations, radiation dose rate values of 20 steps are collected by ENSAW algorithm as the input data for CNN pre-training, that is, the network model has been trained before the searcher is scheduled.

3. The ACA algorithm

3.1. Source parameter estimation based on convolutional neural network

The direction and location of the radioactive source is initially unknown for searcher, and the search for radioactive source is a gradual process. However, existing source parameter estimation models are difficult to accurately estimate the source parameters in

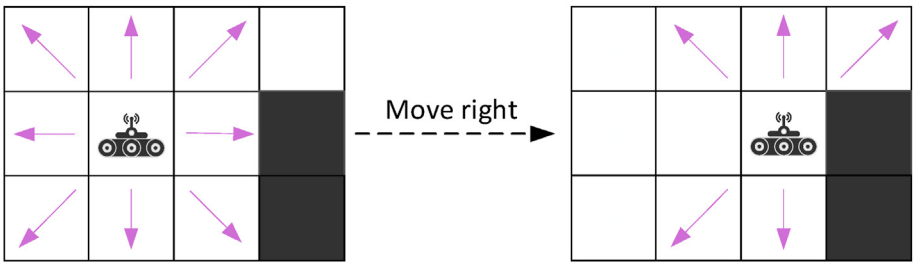

Fig. 3. Collect radiation data in occupied grid map. The blank grid represents the unoccupied grid; the black grid represents the occupied grid; the pink arrow indicates the direction which searcher may choose to move next. (For interpretation of the references to colour in this figure legend, the reader is referred to the Web version of this article.)

indoor environments with obstacles. Therefore, in this study, convolutional neural network (CNN) algorithm is used for the parameter estimation of radioactive source. CNN is widely used in image classification and cognition, machine vision, natural language processing and other fields. Not long ago, Fathi et al. [18] and Hu et al. [27] used CNN to predict the location of radioactive sources, which can locate the location of single or multiple radioactive sources with sparse measurement data. However, when the number of grids and the potential location of source are large, the estimation accuracy of the network model will decline rapidly and the overfitting occurs in training. In order to solve these problems, this paper introduces "Dropout" and adjusts the superparameters of the full connection layer to increase the estimation accuracy of source location, avoid overfitting of CNN and reduce the training time [28–30]. Also, a path planning algorithm based on heuristic search is selected and introduced to make the optimal decision at the current state in Section 3.2.

In Section 2.2, the radiation dataset is obtained by the ENSAW algorithm. Next, the radiation dataset is randomly divided into training set, verification set according to the ratio of 96.5 : 3.5. Among them, the training set is used to fit the classification model, and the validation set is used to adjust the hyperparameters of the model and conduct a preliminary evaluation of the performance of the network model. The designed CNN architecture is shown in Fig. 4. The CNN architecture uses three layers of convolutional layers to extract radiation features, and three layers of full connections form an artificial neural network for source location classification. After the radiation feature extraction is completed, the convolution result is flattened into a long vector composed of 117504 neurons, which will be used as the input layer of the artificial neural network. However, if each neuron in the long vector is directly connected to each neural source of the fully connected layer FC4, the total trainable parameters will exceed 70 million, resulting in over-fitting of the network model and a sharp decrease in classification accuracy. Therefore, we introduce "Dropout" after 'Flatten' to randomly deactivate neurons with a probability of 30%, which will avoid over-fitting of the network model and increasing the accuracy of source location estimation.

3.2. Path planning based on A-star algorithm

To solve the problem that the features of randomly collected radiation data in the search process may not be extracted by the network model, we introduce A-star algorithm to plan source search path and guide the direction of radiation collection. A-star algorithm is often used in mobile robot's path planning in robot field [21], and can minimize the sensor operations to reduce time consumption [31]. Unlike non-heuristic search [32], A-star algorithm combines Dijkstra algorithm with breadth first search (BFS) algorithm through heuristic search, and uses cost estimation function as the basis of path search to obtain the optimal path. The cost estimation function can be expressed as:

$$f(n) = g(n) + h(n) \tag{6}$$

Where, n represents the current node in the path search process; $f(n)$ represents the total cost of the starting position node to reach the target node through the current position node; $g(n)$ represents

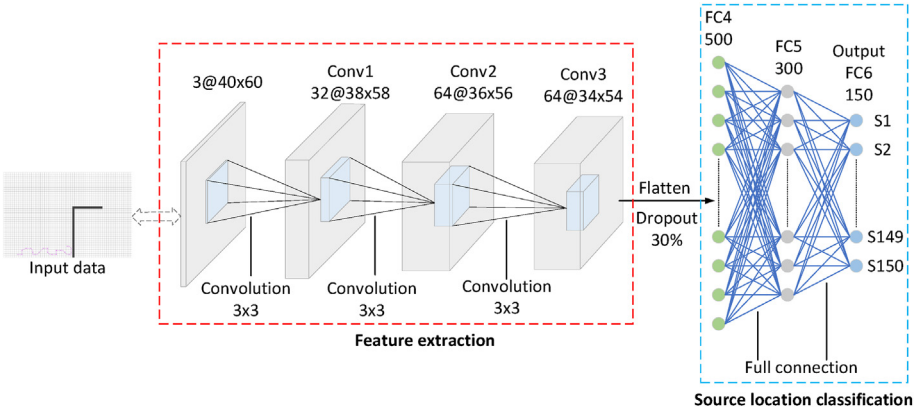

Fig. 4. The design of convolutional neural network architecture. Conv1, Conv2 and Conv3 represent convolutional layers, and FC4, FC5 and FC6 represent fully connected layers. The first layer is the input layer. The input data is expanded into three-channel. The convolution kernel size of the convolutional layer Conv1 is 3 × 3, and the number of channels is 32. The convolution kernel size of the convolutional layers Conv2 and Conv3 is 3 × 3, and the number of channels is 64. FC4, FC5 and FC6 are fully connected layers, and the number of neurons in each layer is 500, 300 and 150, respectively. S1~S150 represent 150 source location classification labels. The activation functions of the convolutional layers Conv1, Conv2, Conv3 and the fully connected layers FC4 and FC5 all use the ReLu activation function which is defined as $f(x) = max(0,x)$. The activation function of the output layer FC6 uses the Softmax activation function, which is defined as $Softmax(x_i) = \frac{e^{x_i}}{\sum_{j=1}^{k} e^{x_j}}$. Adam is chosen as the optimizer for the network.

the actual cost from the starting point node to the current location node; $h(n)$ represents the valuation cost from the current location node to the destination node. The starting position coordinate is (x_1, y_1), and the current position coordinate is (x_i, y_i). Let the coordinate of the target point is (x_g, y_g). Then, the actual cost $g(n)$ is calculated by the following formula:

$$g(n) = \sum_{k=1}^{p-1} d(k) \tag{7}$$

Where, p is the number of grids from the starting grid to the current grid ($p \geq 1$); $d(k)$ is the Euclidean distance from the k th grid to the $k+1$ th grid. Let the coordinates of the k th grid and $k+1$ th grid be (x_k, y_k), (x_{k+1}, y_{k+1}) respectively, then $d(k)$ can be expressed as:

$$d(k) = \sqrt{(x_k - x_{k+1})^2 + (y_k - y_{k+1})^2} \tag{8}$$

$h(n)$ is calculated by Manhattan distance, and the Manhattan distance between the current position and the target position is expressed as:

$$h(n) = |x_i - x_g| + |y_i - y_g| \tag{9}$$

In the process of radioactive source search, initially, since the location of radioactive source is unknown to the searcher, it is indispensable to randomly collect radiation data and feed them into the network model to predict the location of radioactive source. Then, the predicted source location is taken as the target point, and A-star algorithm is used to plan the search path. Further, the radiation data collected under the planned search path (including the previously collected radiation data) will be input into the CNN model to update the predicted location of source. The process is iterated until the searcher successfully reaches the location of source. The flow chart of radioactive source search based on ACA algorithm is shown in Fig. 5.

4. Results and discussion

In order to verify the feasibility and high efficiency of the ACA algorithm for source search, verification experiments were carried out in open indoor environment and indoor environment with obstacle. We also compared the number of radiation measurements, the number of moving steps, and search success rate with existing GS algorithm which is implemented by Liu et al. [17], and extended the gradient search direction from four-neighbor to eight-neighbor. The GS algorithm can guide the searcher to move in the direction of rising radiation gradient. The radiation gradient is defined as $\frac{d_m}{dl}$, where d_m is the change of radiation measurement and dl is the change of the measurement position. The radiation gradients in the eight-neighbor search directions are expressed as $(g_1, g_2, g_3, g_4, g_5, g_6, g_7, g_8)$; g_1, g_2, g_3, g_4, g_5, g_6, g_7 and g_8 represent the radiation gradients in the eight-neighbor search direction. In order to prevent the searcher from only moving in the direction of the fastest rising radiation gradient, the radiation gradient is converted into a moving probability vector, and then an adjustment factor q is introduced to control the randomness of the next move decision.

$$(q_1, q_2, q_3, q_4, q_5, q_6, q_7, q_8) = softmax\left(\frac{g_1}{q}, \frac{g_2}{q}, \frac{g_3}{q}, \frac{g_4}{q}, \frac{g_5}{q}, \frac{g_6}{q}, \frac{g_7}{q}, \frac{g_8}{q}\right) \tag{10}$$

The larger the q value, the more random the direction of movement will be; the smaller the q value, the greater the probability that the searcher will move to the direction where the radiation gradient rises fastest. The best q value has been determined through countless experiments: the q value is set as 0.8 in an open indoor environment, and the q value is set as 1.6 in an indoor environment with obstacle. In addition, in order to facilitate the comparison with the proposed algorithm and avoid the randomness of the experiment, for the GS algorithm, we repeated the experiment 100 times and chose the optimal result to compare with the proposed algorithm.

4.1. Experiment and analysis in open indoor environment

The radiation dataset obtained by the ENSAW algorithm in Section 2.2 is divided proportionally and then fed into the designed network architecture (Fig. 4) for training. The curves of training accuracy, verification accuracy, training loss and verification loss are shown in Fig. 6. Both training accuracy and training loss have

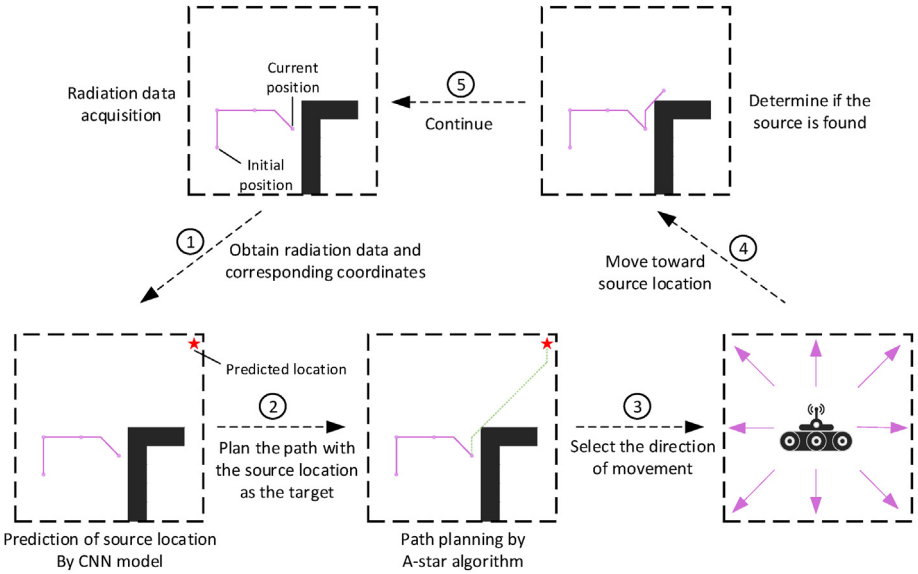

Fig. 5. Flow chart of radioactive source search based on ACA algorithm.

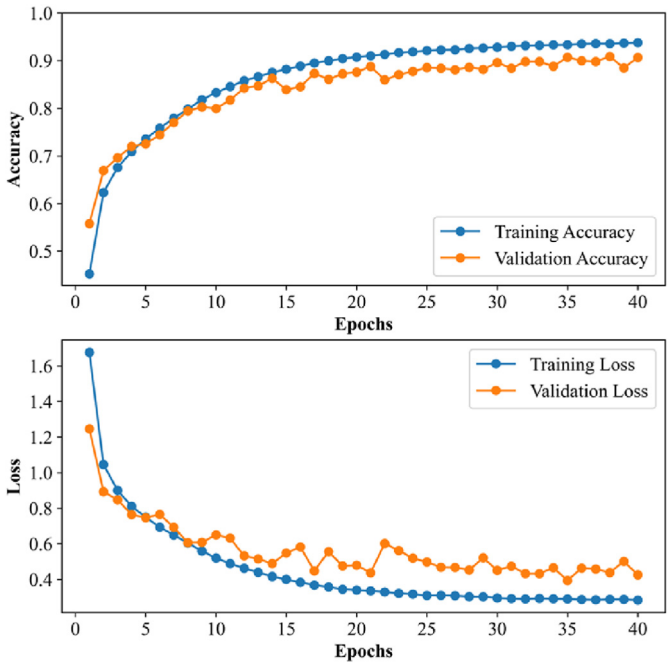

Fig. 6. Training curves of the network model.

converged after 40 epochs, and the verification accuracy and verification loss are close to the training accuracy and training loss, respectively.

In order to evaluate the performance of the network model and analyze the prediction results, randomly select 10 different source locations and use the ENSAW algorithm to generate radiation dose rate values of 20 steps with 10000 new radiation data. Further, the first three source locations with higher probability predicted by the network model and their corresponding probabilities are statistically analyzed (Table 1). It can be seen from Table 1 that although the prediction result may not be consistent with the actual location of radioactive source, most of the incorrectly predicted source locations are still around the actual source location (the eight cells adjacent to the actual cell). For example, when the actual location of source is at S29, the incorrectly predicted locations S13 and S28 are at the upper left corner and the left side, respectively. In addition, a small number of prediction results seriously deviate from the actual source location. The reason is that the network fails to extract radiation features due to the influence of radiometric data, which leads to misclassification of source location.

In order to make up for the above shortcomings, the A-star algorithm is introduced to plan the searcher's walking path and guide the direction of radiation data collection. Since the location of radioactive source is unknown at the beginning of the search, random radiation data collection is required to estimate the direction of source. Then, source location is estimated every four radiation data acquisitions in the occupancy grid map, so that the searcher can adjust the search direction in time and conduct a gradual search towards the source location. Fig. 7 shows the comparison experiment of ACA algorithm and GS algorithm for source search in open indoor environment. Table 2 shows the estimated source location of source parameter estimation model during the search process. In plot (a) of Fig. 7, the first three estimation results of the source parameter estimation model of the ACA algorithm are all at or around the actual source location. The walking path is planned by the A-star algorithm so that the searcher that collects radiation data at a fixed step distance of 0.5 m moves towards the source location. However, an error occurs at the fourth estimate, causing the searcher to move away from the actual source location. The fifth and subsequent estimates are all correct. In the end, the radioactive source is successfully found.

Table 1
Analysis of prediction results of source parameter estimation model.

Actual source location	Estimated source location			Corresponding probability		
S15	S15	S14	S90	95.0%	0.5%	0.5%
S29	S29	S13	S28	88.9%	1.4%	1.3%
S43	S43	S42	S27/S59	92.4%	0.9%	0.8%
S57	S57	S72	S41	91.3%	1.5%	1.2%
S71	S71	S86	S56	93.1%	1.9%	1.1%
S85	S85	S86	S70	91.2%	1.6%	1.5%
S99	S99	S114	S84	91.3%	2.4%	1.3%
S113	S113	S98	S114	87.2%	4.2%	2.4%
S127	S127	S128	S143	91.6%	1.4%	1.2%
S141	S141	S140	S142	90.0%	2.3%	1.9%

In plot (b) of Fig. 7, although there is a large deviation between the estimated source location for the first time and the actual source location, the second estimation result is the actual source location, which enables the searcher to adjust the search direction in time and plan the optimal path. The results of the fourth and subsequent estimates are all correct, and the radioactive source is also successfully searched in the end. In contrast, the GS algorithm needs to collect radiation data in eight directions for each moving step and make a decision through formula (10) to select the next moving direction, which will lead to low search efficiency. Although both the ACA algorithm and the GS algorithm can successfully search for radioactive source in the end, the average number of radiation measurements of the ACA algorithm is only 2.1% of that of the GS algorithm. In addition, the average number of moving steps of the ACA algorithm is only 33.2% of that of the GS algorithm.

4.2. Experiment and analysis in indoor environment with obstacle

In Section 4.1, source search experiments in an open indoor environment are carried out using the ACA algorithm. However, there may be concrete wall that blocks the radiation signal during the indoor source search process, which may interfere with the source location estimation. Considering an L-shaped concrete wall in an indoor environment, similarly, the detector acquisition plane is represented by an occupancy grid map. Further, the radiation dose rate distribution maps at the height of 1 m above the ground for different source locations are approximated by the Geant4 program based on the MC method (Fig. 8).

Similar to Section 4.1, the ENSAW algorithm is used to collect radiation data of 20 steps in the occupancy grid map, and 600,000 radiation data are collected for the radiation dose rate distribution maps of different source locations as the data set. The data set is divided according to the same ratio and then fed into the same network architecture for training. The training results are shown in Fig. 9. The training accuracy and training loss have converged approximately after 40 epochs, and the verification accuracy and verification loss are close to the training accuracy and training loss, respectively, indicating that the source parameter estimation model is also suitable for estimating the source location in the indoor environment with obstacles.

In the same way, 10 different radiation source locations were selected, and then 10,000 new radiation data of 20 steps were randomly generated using the ENSAW algorithm to evaluate the performance of the network model and analyze the prediction results. Next, the first three source locations with higher probability predicted by the network model and their corresponding

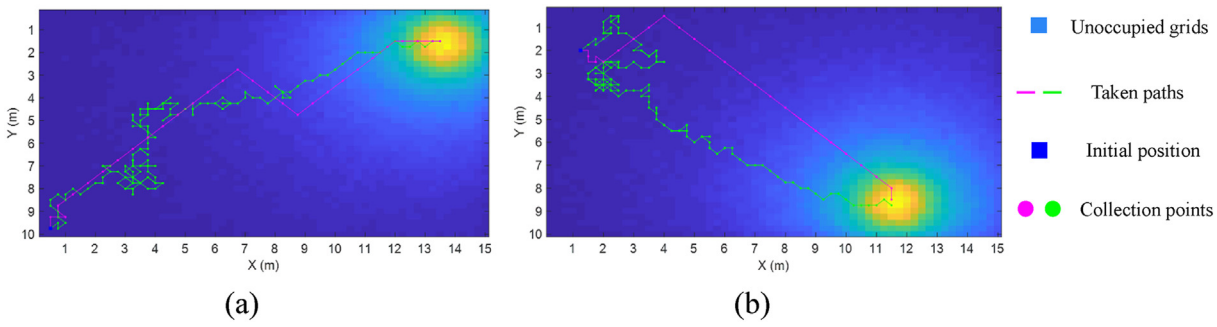

Fig. 7. Comparison experiment of radioactive source search between ACA algorithm (magenta) and GS algorithm (green). (a) The radioactive source is located in the upper right corner, and the initial position of the searcher is in the lower left corner. (b) The radioactive source is located in the lower right corner, and the initial position of the searcher is in the upper left corner. (For interpretation of the references to colour in this figure legend, the reader is referred to the Web version of this article.)

Table 2
Estimated source location of ACA algorithm.

No.	Actual source location	Estimated source location							
		1st	2nd	3rd	4th	5th	6th	7th	8th
(a)	S29	S15	**S29**	S45	S89	**S29**	**S29**	**S29**	**S29**
(b)	S132	S14	**S132**	S104	**S132**	**S132**	**S132**	/	/

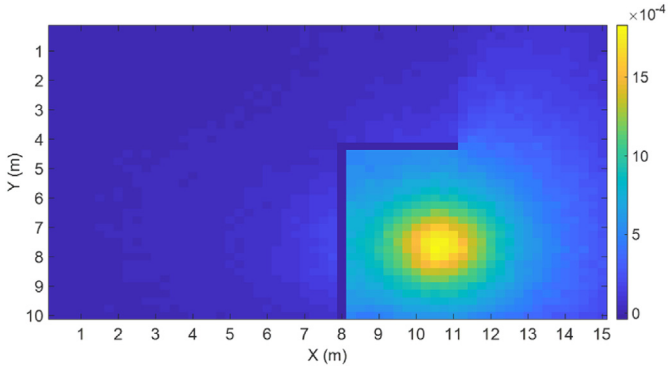

Fig. 8. Radiation dose rate distribution map of radioactive source (S116) at the height of 1 m above the ground (dose rate: μGy/s).

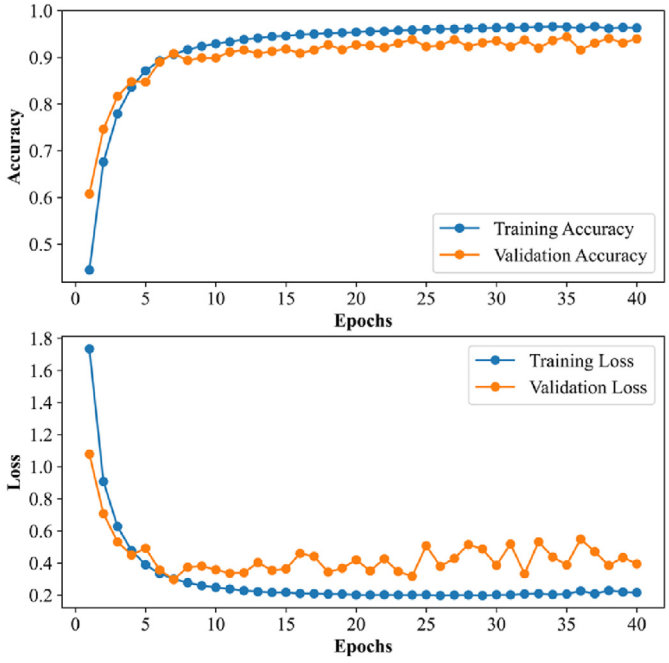

Fig. 9. Training curves of the network model.

probabilities are statistically analyzed (Table 3). It can be seen from Table 3 that although the indoor concrete wall will block the radiation signal, most of the wrongly estimated source locations are still around the actual source location by source parameter estimation model. For example, when the radioactive source is located at location S29, the wrongly estimated locations S28 and S30 are on its left and right, respectively. In addition, a small number of prediction results seriously deviate from the actual location of radioactive source. This is mainly related to the fact that the radiation signal is blocked by concrete wall and the location of radiation measurements, so that the network fails to extract radiation features, which leads to misclassification of source location. Thus, the A-star algorithm is introduced to plan the searcher's walking path and guide the direction of radiation data collection. In addition, during the search process, the A-star algorithm can avoid obstacles and make optimal path planning between the current position and the target position.

In order to prove the feasibility and efficiency of the ACA algorithm in indoor environment with obstacles, a series of source search simulation experiments have been carried out. Fig. 10 shows the source search process of ACA algorithm and GS algorithm. Table 4 shows the location estimation results of the source parameter estimation model of ACA algorithm. In plot (a) of Fig. 10,

Table 3
Analysis of prediction results of source parameter estimation model.

Actual source location	Estimated source location			Corresponding probability		
S15	S15	S30/S75	S57	94.0%	1.2%	0.7%
S29	S29	S28	S30	87.2%	2.9%	2.1%
S43	S43	S28	S42	89.2%	2.1%	1.9%
S57	S57	S42	S12	96.9%	0.6%	0.4%
S71	S71	S86	S85	93.6%	1.1%	0.7%
S85	S85	S70/S100	S99	96.1%	0.7%	0.4%
S99	S99	S84/S100	S114	94.2%	1.1%	0.8%
S113	S113	S98	S127	86.9%	3.1%	2.2%
S127	S127	S126	S128	89.9%	3.4%	2.1%
S141	S141	S140	S127	88.6%	3.2%	1.7%

the radioactive source is located inside the wall, and the initial position of the searcher is in the lower left corner. The first estimation result of the source parameter estimation model was close to the actual source location. Then, with the estimated source location as the target, path planning was made between the current state and the target by A-star algorithm, and radiation data was collected with a fixed step distance. However, the second

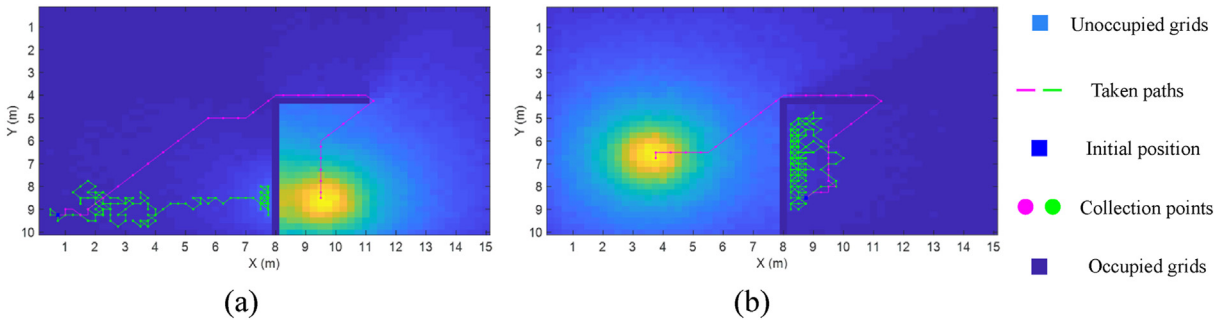

Fig. 10. Comparison experiment of ACA algorithm (magenta) and GS algorithm (green) for radioactive source search. (a) The radiation source is located inside the wall, and the initial position of the searcher is in the lower left corner. (b) The radiation source is located outside the wall, and the initial position of the searcher is inside the wall. (For interpretation of the references to colour in this figure legend, the reader is referred to the Web version of this article.)

Table 4
Estimated source location of ACA algorithm.

No.	Actual source location	Estimated source location							
		1st	2nd	3rd	4th	5th	6th	7th	8th
(a)	S130	S101	S27	**S130**	**S130**	**S130**	**S130**	**S130**	**S130**
(b)	S94	S109	S64	**S94**	S78	**S94**	**S94**	**S94**	/

estimation result deviated severely from the actual source location, resulting in the failure of optimal path planning. Subsequently, the location of source was correctly estimated in the third estimate, and the direction of movement was corrected in time. Ultimately, the searcher successfully found the radioactive source using the ACA algorithm with 62 moving steps and 31 radiation measurements. On the contrary, the GS algorithm eventually fails to search the source due to being trapped in a local optimum.

In plot (b) of Fig. 10, the radiation source is located outside the wall, and the initial position of the searcher is inside the wall. The source parameter estimation model of ACA algorithm only deviates from the actual source location for the second estimate, and the rest of the estimation results are all correct or around the actual source location. Also, the A-star algorithm is used to plan the optimal path between the current position and the target position. In the end, the searcher successfully arrived at the location of radioactive source with 52 moving steps and 26 radiation measurements. However, the GS algorithm makes the searcher always move on the inner side of the wall and collect radiation data, so that the searcher fails to go around the wall and is finally trapped a local optimum. The experimental results show that in the indoor environment with obstacle, the ACA algorithm is significantly better than the GS algorithm in the number of moving steps, the number of radiation measurements and the success rate of source search.

5. Conclusion

In this paper, a novel automatic search algorithm (ACA algorithm) for radioactive source based on CNN and A-star algorithm is proposed to solve the problem of low efficiency of mobile robots searching for radioactive source in indoor environments without and with obstacles. Through an iterative process of source location estimation and path planning, the progressive search for radioactive source is realized. The feasibility and effectiveness of ACA algorithm are verified by comparative experiments in approximate real indoor scenes. The experimental results show that in the open indoor environment, the average number of radiation measurements and the average number of moving steps of the ACA algorithm are 2.1% and 33.2% of the GS algorithm, respectively. In the indoor environment with obstacles, the GS algorithm will fall into a local optimum due to the wall blocking the radiation signal, resulting in the failure of the source search, while the ACA algorithm is significantly better than the GS algorithm in the number of moving steps, the number of radiation measurements, and the success rate of source search. However, the proposed algorithm may fail to search for source in complex geometric environments due to the limitations of the source parameter estimation model. In the future, we would like to conduct experiments in more complex indoor environments including terrain constraints to improve the proposed algorithm. In particular, when the search area is large enough, multiple robots can be employed to search for radioactive source to further improve search efficiency [33]. In addition, during the source search process, the radiation dose rate map in the region or space can be reconstructed or inverted to better solve the problem of automatic search for radioactive source.

Declaration of competing interest

The authors declare that they have no known competing financial interests or personal relationships that could have appeared to influence the work reported in this paper.

Acknowledgments

This research was funded by the National Natural Science Foundation of China (No.12205245, No.12175187), Natural Science Foundation of Sichuan Province (No. 2023NSFSC1437), Research Fund of Southwest University of Science and Technology (No. 22zx7109).

References

[1] IAEA Incident and Trafficking Database (ITDB), Incidents of nuclear and other radioactive material out of regulatory control, Available online: https://www.iaea.org/sites/default/fifiles/22/01/itdb-factsheet.pdf. (Accessed 17 November 2022).
[2] A.H.W. Liu, Simulation and Implementation of Distributed Sensor Network for Radiation Detection, California Institute of Technology, 2010.
[3] N.S.V. Rao, M. Shankar, J.C. Chin, D.K. Yau, S. Srivathsan, S.S. Iyengar, Identification of Low-Level Point Radiation Sources Using a Sensor Network. 2008 International Conference on Information Processing in Sensor Networks (IPSN), IEEE, 2008, pp. 493–504, 2008.
[4] J.W. Howse, L.O. Ticknor, K.R. Muske, Least squares estimation techniques for

position tracking of radioactive sources, Automatica 37 (11) (2001) 1727–1737.
[5] Y. Huang, J. Benesty, G.W. Elko, R.M. Mersereati, Real-time passive source localization: a practical linear-correction least-squares approach, IEEE Trans. Speech Audio Process. 9 (8) (2001) 943–956.
[6] A. Gunatilaka, B. Ristic, R. Gailis, On Localisation of a Radiological Point Source. 2007 Information, Decision and Control, IEEE, 2007, pp. 236–241, 2007.
[7] E. Bai, A. Heifetz, P. Raptis, S. Dasgupta, R. Mudumbai, Maximum likelihood localization of radioactive sources against a highly fluctuating background, IEEE Trans. Nucl. Sci. 62 (6) (2015) 3274–3282.
[8] H.E. Baidoo-Williams, Maximum Likelihood Localization of Radiation Sources with Unknown Source Intensity, 2016 arXiv preprint arXiv:1608.00427.
[9] J. Huo, M. Liu, K.A. Neusypin, H. Liu, M. Guo, Y. Xiao, Autonomous search of radioactive sources through mobile robots, Sensors 20 (12) (2020) 3461.
[10] Y. Liu, Y. Xuan, D. Zhang, S. Zou, Localizing unknown radiation sources by unscented particle filtering based on divide-and-conquer sampling, J. Nucl. Sci. Technol. (2022) 1–13, 2022.
[11] W. Gao, W. Wang, H. Zhu, G. Huang, D. Wu, Z. Du, Robust radiation sources localization based on the peak suppressed particle filter for mixed multi-modal environments, Sensors 18 (11) (2018) 3784.
[12] M.R. Morelande, B. Ristic, Radiological source detection and localisation using Bayesian techniques, IEEE Trans. Signal Process. 57 (11) (2009) 4220–4231.
[13] A. West, I. Tsitsimpelis, M. Licata, A. Jazbec, L. Snoj, M.J. Joyce, B. Lennox, Use of Gaussian process regression for radiation mapping of a nuclear reactor with a mobile robot, Sci. Rep. 11 (1) (2021) 1–11.
[14] X. Xie, J. Cai, Z. Tang, The reconstruction of 3D radiation field based on sparse measurement data, Ann. Nucl. Energy 179 (2022), 109391.
[15] H. Tomita, S. Hara, A. Mukai, K. Yamagishi, H. Ebi, K. Shimazoe, Y. Tamura, H. Woo, H. Takahashi, H. Asama, F. Ishida, E. Takada, J. Kawarabayashi, K. Tanabe, K. Kamada, Path-planning system for radioisotope identification devices using 4π gamma imaging based on random forest analysis, Sensors 22 (12) (2022) 4325.
[16] M.S. Lee, M. Hanczor, J. Chu, Z. He, N. Michael, R. Whittaker, 3-d Volumetric Gamma-Ray Imaging and Source Localization with a Mobile Robot, 2018 arXiv preprint arXiv:1802.06072.
[17] Z. Liu, S. Abbaszadeh, Double Q-learning for radiation source detection, Sensors 19 (4) (2019) 960.
[18] A. Fathi, S.F. Masoudi, Lost gamma source detection algorithm based on convolutional neural network, Nucl. Eng. Technol. 53 (11) (2021) 3764–3771.
[19] Y. Zhao, B. Chen, X.H. Wang, Z. Zhu, Y. Wang, G. Cheng, Y. Liu, A deep reinforcement learning based searching method for source localization, Inf. Sci. 588 (2022) 67–81.
[20] P. Proctor, C. Teuscher, A. Hecht, M. Osiński, Proximal policy optimization for radiation source search, Journal of Nuclear Engineering 2 (4) (2021) 368–397.
[21] J. Chen, C. Tan, R. Mo, H. Zhang, G. Cai, H. Li, Research on path planning of three-neighbor search A* algorithm combined with artificial potential field, Int. J. Adv. Rob. Syst. 18 (3) (2021), 17298814211026449.
[22] Y. Ji, Y. Zhao, B. Chen, Z. Zhu, Y. Liu, H. Zhu, S. Qiu, Source searching in unknown obstructed environments through source estimation, target determination, and path planning, Build. Environ. 221 (2022), 109266.
[23] S. Agostinelli, J. Allison, K.A. Amako, J. Apostolakis, H. Araujo, P. Arce, Geant4 Collaboration., GEANT4—a simulation toolkit, Nucl. Instrum. Methods Phys. Res. Sect. A Accel. Spectrom. Detect. Assoc. Equip. 506 (3) (2003) 250–303.
[24] J.F. Briesmeister, MCNPTM-A General Monte Carlo N-Particle Transport Code, in: Version 4C, LA-13709-M, vol. 2, Los Alamos National Laboratory, 2000.
[25] A. Ferrari, J. Ranft, P.R. Sala, A. Fassò, FLUKA: A Multi-Particle Transport Code (Program Version 2005), Cern, 2005.
[26] M. Bousquet-Mélou, On the importance sampling of self-avoiding walks, Combinator. Probab. Comput. 23 (5) (2014) 725–748.
[27] X. Hu, J. Huo, J. Wang, L. Hu, Y. Xiao, Research on a localization method of multiple unknown gamma radioactive sources, Ann. Nucl. Energy 177 (2022), 109302.
[28] A. Krizhevsky, I. Sutskever, G.E. Hinton, Imagenet classification with deep convolutional neural networks, Commun. ACM 60 (6) (2017) 84–90.
[29] K. Simonyan, A. Zisserman, Very Deep Convolutional Networks for Large-Scale Image Recognition, 2014 arXiv preprint arXiv:1409.1556.
[30] N. Srivastava, G. Hinton, A. Krizhevsky, I. Sutskever, R. Salakhutdinov, Dropout: a simple way to prevent neural networks from overfitting, J. Mach. Learn. Res. 15 (1) (2014) 1929–1958.
[31] N.S.V. Rao, On performance of path planning algorithms in unknown terrains, ORSA J. Comput. 4 (2) (1992) 218–224.
[32] N.S.V. Rao, S. Kareti, W. Shi, S.S. Iyengar, Robot Navigation in Unknown Terrains: Introductory Survey of Non-heuristic Algorithms, Oak Ridge National Lab., TN (United States), 1993.
[33] M. Ling, J. Huo, G.V. Moiseev, L. Hu, Y. Xiao, Multi-robot collaborative radioactive source search based on particle fusion and adaptive step size, Ann. Nucl. Energy 173 (2022), 109104.